

Magnetic excitations in molecular magnets with complex bridges: The tetrahedral molecule $\text{Ni}_4\text{Mo}_{12}$

M. Georgiev* and H. Chamati

Institute of Solid State Physics, Bulgarian Academy of Sciences, Tsarigradsko Chaussée 72, 1784 Sofia, Bulgaria
(Dated: January 20, 2022)

We investigate the spectroscopic magnetic excitations in molecular magnets with complex intermediate structure among the magnetic ions. Our approach consists in introducing a modified spin Hamiltonian that allows for discrete coupling parameters accounting for all energetically favorable spatial distributions of the valence electrons along the exchange bridges connecting the constituent magnetic ions. We discuss the physical relevance of the constructed Hamiltonian and derive its eigenvalues. The model is applied to explore the magnetic excitations of the tetrameric molecular magnet $\text{Ni}_4\text{Mo}_{12}$. Our results are in a very good agreement with the available experimental data. We show that the experimental magnetic excitations in the named tetramer can be traced back to the specific geometry and complex chemical structure of the exchange bridges leading to the splitting and broadness of the peaks centered about 0.5 meV and 1.7 meV.

PACS numbers: 75.10.-b, 75.10.Jm, 75.30.Et, 75.50.-y, 75.50.Xx

I. INTRODUCTION

The physical properties, such as energy spectra, susceptibility, etc., of magnetic clusters at the nanoscale depend on their size, shape and the presence of different bondings among the constituent chemical elements and thus the distribution of ligands between the magnetic ions (for more details see¹⁻⁴ and references therein). Some prominent examples are Mn based magnetic compounds⁵⁻¹¹ and spin clusters with Ni magnetic ions¹²⁻¹⁵.

Magnetic molecules possess unique properties that can be characterized with great accuracy both experimentally and theoretically. Thus they are ideal tools to gain useful insights into the underlying coupling mechanisms. The study of basic units like tetramers^{16,17} prove the importance of analytical methods in revealing the role of electrons correlations underpinning molecular magnetism. On the experimental side, Inelastic Neutron Scattering (INS)¹⁸⁻²¹ plays a central role in determining the relevant magnetic spectra. In complement to different magnetic measurement methods, INS technique appears to be essential, and in the past decades it has been widely applied to explore the properties of spin clusters. Experiments on the spin dimer $[\text{Ni}_2(\text{ND}_2\text{C}_2\text{H}_4\text{ND}_2)_4\text{Br}_2]\text{Br}_2$ have demonstrated the important contribution of neutron spectroscopy²². INS measurements were obtained for different magnetic clusters, such as: The trimer $\text{La}_4\text{Cu}_3\text{MoO}_{12}$, with strong intratrimer antiferromagnetic interactions, where the copper ions form an isolated triangle²³, the Fe based molecular wheel with eighteen spin- $\frac{5}{2}$ ions²⁴, the dimer $\text{SrCu}_2(\text{BO}_3)_2$ with observed multiplet excitations^{25,26}, the polyoxomolybdate $\text{Mn}_{72}\text{Fe}_{32}$ ²⁷, and the magnetic molecule Fe_9 in the presence of an external magnetic field²⁸.

In the present work we propose an approach based on the assumption that in a molecular magnet with multiple exchange bridges between any two magnetic centers (ions) the distribution of unpaired valence electrons is not unique. Thus, the electron's density distribution might vary among the existing exchange bridges affecting the transition energy, and consequently leading to either a broadened excitation width or split-

ting in the energy spectrum. Accordingly the number of all energy levels form a set that can utterly identify the most relevant spin bonds, despite being indistinguishable. To this end, we introduce a modified microscopic spin Hamiltonian with discrete couplings that incorporates distinct spin coupling mechanisms among equivalent spins allowing one to identify the different exchange paths. The proposed Hamiltonian leads to an unperturbed energy structure that distinguish the relevant magnetic features from those arising due the magnetic anisotropy. It is worth mentioning that the present approach was successfully applied to the study of the magnetic excitations in the trimers $\text{A}_3\text{Cu}_3(\text{PO}_4)_4$ with ($\text{A} = \text{Ca}, \text{Sr}, \text{Pb}$)²⁹.

Here, the present method will be validated by reproducing the experimentally obtained INS spectrum of a molecular magnet that has generated a great deal of interest among researchers both on the theoretical, as well as the experimental sides. This is the magnetic molecule $[\text{Mo}_{12}\text{O}_{30}(\mu_2\text{-OH})_{10}\text{H}_2(\text{Ni}(\text{H}_2\text{O})_3)_4]$, denoted by $\text{Ni}_4\text{Mo}_{12}$, where four spin-1 Ni^{2+} ions are sitting on the vertices of a distorted tetrahedron³⁰. We would like to point out that previous studies^{31,32} did not succeed to obtain the main peaks and the broadening in the INS spectrum, see FIG. 1, despite including single-ion anisotropy or higher-order terms in the Heisenberg model with nearest-neighbor interaction or even using the Hubbard model.

II. THE MODEL AND THE METHOD

In order to identify the experimentally observed magnetic peaks, see FIG. 1, one has to calculate the scattering intensities $I_{n'n}(\mathbf{q})$, of the existing transitions and analyse their dependence on the temperature and the magnitude of the neutron scattering vector. For identical magnetic ions, we have¹⁸⁻²¹

$$I_{n'n}(\mathbf{q}) \propto F^2(\mathbf{q}) \sum_{\alpha, \beta} \Theta^{\alpha\beta} S^{\alpha\beta}(\mathbf{q}, \omega_{n'n}). \quad (2.1)$$

Here $\omega_{n'n}$ is the transition frequency, \mathbf{q} is the scattering vector, $F(\mathbf{q})$ is the spin magnetic form factor³³, $\Theta^{\alpha\beta}$ are the elements

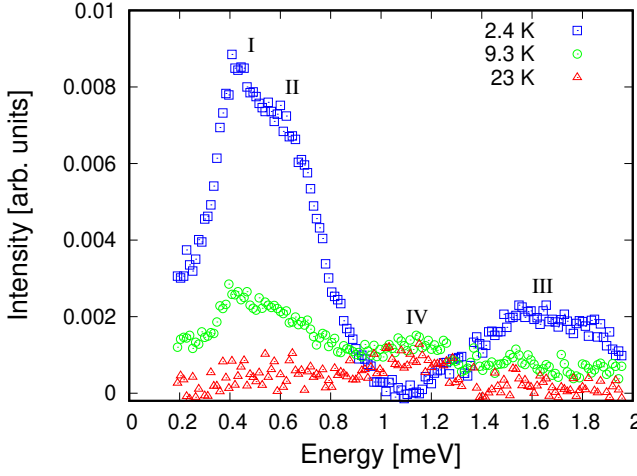


FIG. 1. Background corrected data for the INS spectrum of the polycrystalline $\text{Ni}_4\text{Mo}_{12}$ taken from Ref.³¹.

of polarization factor, $S^{\alpha\beta}(\mathbf{q}, \omega_{n'n})$ are the magnetic scattering functions and $\alpha, \beta, \gamma \in \{x, y, z\}$.

To determine the energy level structure and the transitions corresponding to the experimentally observed magnetic spectra one needs a minimal number of parameters to account for all couplings in the system. The principal assumption is that the magnetic excitations of spin clusters obtained via INS are mainly governed by the exchange of electrons between effective spin magnetic centers. Then, the experimental data are interpreted in terms of a well defined microscopic spin model. In the absence of anisotropy, i.e. negligible spin-orbit coupling, the exchange interaction in molecular magnets can be described by the Heisenberg model

$$\hat{H} = \sum_{i \neq j} J_{ij} \hat{\mathbf{s}}_i \cdot \hat{\mathbf{s}}_j, \quad (2.2)$$

where $J_{ij} = J_{ji}$ is the exchange coupling that effectively accounts for the exchange interaction between the i th and j th ions. However, to distinguish all magnetic excitations one has to use an appropriate spin model leading to an energy sequence such that the scattering functions in (2.1) identifies the relevant spin bonds. Therefore, even with a selected *a priori* spin coupling scheme for a cluster with complex intermediate structure Hamiltonian (2.2) may not be fully adequate to obtain the correct energy structure.

A. The effective spin Hamiltonian

In order to characterize uniquely each pair of magnetic centers in a magnetic cluster, bonded via more than one intermediate bridge, we propose the following Hamiltonian

$$\hat{\mathcal{H}} = \sum_{i \neq j} J_{ij} \hat{\sigma}_i \cdot \hat{\sigma}_j, \quad (2.3)$$

where the couplings $J_{ij} = J_{ji}$ are effective exchange constants and the operator $\hat{\sigma}_i = (\hat{\sigma}_i^x, \hat{\sigma}_i^y, \hat{\sigma}_i^z)$ accounts for the variation in

valence electron's distribution with respect to the i th magnetic center.

A detailed derivation of the effective Hamiltonian (2.3) is very lengthy and falls beyond the scope of this study (the case of magnetic dimers is published in Ref.³⁴). In the following we will give a brief account of the main steps leading to construct the ensuing Hamiltonian (2.3). Let us point out that our computations are based on the Molecular Orbital Theory³⁵ in terms of the complete active space self consistent field method^{36,37}. We assume that each exchange bridge connecting two magnetic centers possess a number of paired valence electrons, nuclei and thus favor a particular spatial distributions of electrons. The canonical Hamiltonian leading to (2.3) accounts for the kinetic energy, electron-electron and electron-nuclei interactions of all valence electrons within the adiabatic approximation. The electrons are considered as delocalized, occupying molecular orbitals $\phi_{k,m_i}(\mathbf{r}_i)$, $k \in \mathbb{N}$, given by linear combinations of atomic orbitals $\psi_{\mu_{\eta_i}, m_i}^{\eta}(\mathbf{r}_i)$, where \mathbf{r}_i are the coordinates of the i th electron, μ_{η_i} label the electronic shell and subshell with respect to the i th electron and η nucleus, m_i is the spin magnetic quantum number of the i th electron. The state function of each electron configuration is given by a linear combination of Slater determinants (of the orbitals $\phi_{k,m_i}(\mathbf{r}_i)$), where the symmetrization is performed with respect to the spin quantum numbers s_{ij} of all electron pairs. The corresponding basis set gives the number of all probable electrons distributions along all exchange bridges. In the simplest case of N valence electrons with $N-2$ pairs, one of the basis states is written as

$$\Psi_{S,M}^{k,k'}(\mathbf{r}_1, \dots, \mathbf{r}_N) \equiv \sum_{P_{\mathbf{r}_1 \dots \mathbf{r}_N}} c_{\mathbf{r}_{N-1}, \mathbf{r}_N} \prod_i^{\frac{N}{2}-1} \frac{\Phi_{s_{2i-1}, 2i}^i(\mathbf{r}_{2i-1}, \mathbf{r}_{2i})}{\sqrt{2^{\frac{N}{2}} N!}} \times \Psi_{s_{N-1}, N}^{k,k'}(\mathbf{r}_{N-1}, \mathbf{r}_N) |S, M\rangle, \quad (2.4)$$

where the sum runs over all permutations on the set of coordinates $\mathbf{r}_1 \dots \mathbf{r}_N$. Both unpaired electrons occupy k th and k' th molecular orbitals with

$$\Psi_{s_{N-1}, N}^{k,k'}(\mathbf{r}_{N-1}, \mathbf{r}_N) = \frac{1}{\sqrt{2}} [\phi_k(\mathbf{r}_{N-1}) \phi_{k'}(\mathbf{r}_N) + (-1)^{s_{N-1}, N} \phi_{k'}(\mathbf{r}_{N-1}) \phi_k(\mathbf{r}_N)].$$

The remaining, paired electrons, are described by the states

$$\Phi_{s_{2i-1}, 2i}^i(\mathbf{r}_{2i-1}, \mathbf{r}_{2i}) = \frac{1}{2} [\phi_i(\mathbf{r}_{2i-1}) \phi_i(\mathbf{r}_{2i}) + (-1)^{s_{2i-1}, 2i} \phi_i(\mathbf{r}_{2i-1}) \phi_i(\mathbf{r}_{2i})].$$

Moreover, for $i, j = 1, \dots, N$ the permutation coefficients

$$c_{\mathbf{r}_i, \mathbf{r}_j} = (-1)^{i+j+1}, \quad c_{\mathbf{r}_j, \mathbf{r}_i} = (-1)^{s_{N-1}, N} (-1)^{i+j+1},$$

account for the antisymmetry of (2.4) and the spin part is given by

$$|S, M\rangle = \otimes_{i=1}^{\frac{N}{2}} |s_{2i-1}, 2i, m_{2i-1}, 2i\rangle.$$

The effective Hamiltonian accounting for all possible configurations of interactions is built according to the expectation values of the initial Hamiltonian representing all electron-electron and electron-nuclei interactions. The effective state

associated with (2.4) is represented by $|\Psi_{S,M}^\tau\rangle$, where $\tau = (k, k')$. The generic wave function describing the multiple bridged structure includes all probabilities related with the spatial distribution of unpaired electrons. Thus, we may compute the eigenstates of the ensuing spin Hamiltonian in terms of an appropriate linear combination of the effective states. In the case of (2.4), this is given by the superposition

$$|s, m\rangle = \sum_{\tau} c_S^\tau |\Psi_{S,M}^\tau\rangle, \quad (2.5)$$

where τ runs over the number of all existing electrons' configurations that depend on all intermediate bridges and $s = 0, 1$, $m = 0, \pm 1$ are the corresponding effective spin and magnetic quantum numbers, that obey the conservation of angular momentum $S \equiv s$, $M \equiv m$. Further, c_S^τ is the associated probability coefficient that depends on S . The expectation values of the canonical Hamiltonian are a part of the eigenstates relevant to (2.5). Within the framework of the given example they are represented by the sum

$$E_{s,m} = \sum_{\tau} |c_S^\tau|^2 E_{S,M}^\tau. \quad (2.6)$$

The elements in the last sum are functions of the Coulomb U_τ, V_τ , hopping t_τ and direct exchange integrals D_τ relevant to each intermediate bridge. For example,

$$E_{1,M}^\tau = V_\tau - D_\tau, \quad M = 0, \pm 1,$$

$$E_{0,0}^\tau = D_\tau + \frac{U_\tau + V_\tau}{2} - \sqrt{4t_\tau^2 + \frac{(U_\tau - V_\tau)^2}{4}}.$$

Within the effective spin space, determined by s and m , one can account for only one transition with energy $|\Delta E| = |E_{1,m} - E_{0,0}|$ due to the 3-fold degeneracy of the triplet level. However, for different spatial distributions of the considered electrons the values of (2.6) alter and accordingly the energy of the transition changes. Such effect is not related neither to the magnetic anisotropy nor higher order multiple interactions. Therefore, conventional bilinear spin Hamiltonians with only one exchange coupling and additional interacting terms is not able to account for the variation in ΔE .

In order to address these features we introduce Hamiltonian (2.3) that depends upon the parameters described hereafter.

B. Properties of the $\hat{\sigma}$ -operators

For a single spin the square and the z component of each operator $\hat{\sigma}$ are completely determined in the basis of the total spin component \hat{s}^z , such that for all i and $\alpha \in \{x, y, z\}$

$$\hat{\sigma}_i^\alpha |\dots, s_i, m_i, \dots\rangle = a_i^{s_i, m_i} \hat{s}_i^\alpha |\dots, s_i, m_i, \dots\rangle, \quad (2.7)$$

where $a_i^{s_i, m_i} \in \mathbb{R}$. Furthermore, the σ rising and lowering operators obey the equations

$$\hat{\sigma}_i^\pm |\dots, s_i, m_i, \dots\rangle = a_i^{s_i, m_i} \hat{s}_i^\pm |\dots, s_i, m_i, \dots\rangle. \quad (2.8)$$

For all i , the square of σ_i commutes only with its z component. Its eigenvalues depend on m_i and according to (2.7) and (2.8) one can distinguish two cases: (1) $m_i = \pm s_i$; (2) $-s_i < m_i < s_i$, where $s_i \neq 0$, with the respective eigenvalues

$$\left(a_i^{s_i, \pm s_i}\right)^2 s_i^2 + a_i^{s_i, \pm s_i} a_i^{s_i, \pm(s_i-1)} s_i, \quad (2.9a)$$

$$\begin{aligned} & \frac{1}{2} a_i^{s_i, m_i} \left[a_i^{s_i, m_i+1} + a_i^{s_i, m_i-1} \right] s_i (s_i + 1) + (a_i^{s_i, m_i})^2 m_i^2 \\ & - \frac{1}{2} a_i^{s_i, m_i} m_i \left[a_i^{s_i, m_i+1} (m_i + 1) + a_i^{s_i, m_i-1} (m_i - 1) \right]. \end{aligned} \quad (2.9b)$$

On the other hand when the spins of i th and j th magnetic ions are coupled, with total spin operator $\hat{s}_{ij} = \hat{s}_i + \hat{s}_j$, the relation (2.7) enters a more general and complex expression. To explore the properties of the coupled spins one has to work with the total σ -operator $\hat{\sigma}_{ij}$. Its z component and square are completely determined in the basis of the spin operator \hat{s}_{ij}^2 . Similar to eq. (2.7) for all $i \neq j$ and $\alpha \in \{x, y, z\}$, we have

$$\hat{\sigma}_{ij}^\alpha |\dots, s_{ij}, m_{ij}, \dots\rangle = a_{ij}^{s_{ij}, m_{ij}} \hat{s}_{ij}^\alpha |\dots, s_{ij}, m_{ij}, \dots\rangle, \quad (2.10)$$

where $a_{ij}^{s_{ij}, m_{ij}} \in \mathbb{R}$. The corresponding rising and lowering operators obey

$$\hat{\sigma}_{ij}^\pm |\dots, s_{ij}, m_{ij}, \dots\rangle = a_{ij}^{s_{ij}, m_{ij}} \hat{s}_{ij}^\pm |\dots, s_{ij}, m_{ij}, \dots\rangle. \quad (2.11)$$

The eigenvalues of $\hat{\sigma}_{ij}^2$ depend on m_{ij} . Therefore having in mind the following two cases $m_{ij} = \pm s_{ij}$, and $-s_{ij} < m_{ij} < s_{ij}$, where $s_{ij} \neq 0$, the eigenvalues read

$$\left(a_{ij}^{s_{ij}, \pm s_{ij}}\right)^2 s_{ij}^2 + a_{ij}^{s_{ij}, \pm s_{ij}} a_{ij}^{s_{ij}, \pm(s_{ij}-1)} s_{ij}, \quad (2.12a)$$

$$\begin{aligned} & \frac{1}{2} a_{ij}^{s_{ij}, m_{ij}} \left[a_{ij}^{s_{ij}, m_{ij}+1} + a_{ij}^{s_{ij}, m_{ij}-1} \right] s_{ij} (s_{ij} + 1) \\ & + (a_{ij}^{s_{ij}, m_{ij}})^2 m_{ij}^2 - \frac{1}{2} a_{ij}^{s_{ij}, m_{ij}} m_{ij} \\ & \times \left[a_{ij}^{s_{ij}, m_{ij}+1} (m_{ij} + 1) + a_{ij}^{s_{ij}, m_{ij}-1} (m_{ij} - 1) \right]. \end{aligned} \quad (2.12b)$$

The corresponding σ -operators share a single coefficient and for $i \neq j$ and $\alpha \in \{x, y, z\}$, we have

$$\hat{\sigma}_i^\alpha |\dots, s_{ij}, m_{ij}, \dots\rangle = a_{ij}^{s_{ij}, m_{ij}} \hat{s}_i^\alpha |\dots, s_{ij}, m_{ij}, \dots\rangle. \quad (2.13)$$

We further assume that the σ -operators preserve the corresponding spin magnetic moment and for a non coupled spin obey the following constraints

$$\hat{\sigma}_i^z |\dots, s_i, m_i, \dots\rangle = m_i |\dots, s_i, m_i, \dots\rangle, \quad (2.14a)$$

$$\hat{\sigma}_i^2 |\dots, s_i, m_i, \dots\rangle = s_i (s_i + 1) |\dots, s_i, m_i, \dots\rangle. \quad (2.14b)$$

Similarly, when the i th and j th spins are coupled, for all $i \neq j$ we have

$$\hat{\sigma}_{ij}^z |\dots, s_{ij}, m_{ij}, \dots\rangle = m_{ij} |\dots, s_{ij}, m_{ij}, \dots\rangle, \quad (2.15a)$$

$$\hat{\sigma}_{ij}^2 |\dots, s_{ij}, m_{ij}, \dots\rangle = s_{ij}(s_{ij} + 1) |\dots, s_{ij}, m_{ij}, \dots\rangle. \quad (2.15b)$$

Taking into account (2.14) together with expressions (2.9b) for all m_i we have $a_{ij}^{s_i, m_i} = 1$. Further, according to constraints (2.15) and eqs. (2.12) we distinguish three cases:

(1) $s_{ij} \neq 0, m_{ij} \neq 0$: Then, for all m_{ij} , $a_{ij}^{s_{ij}, m_{ij}} = 1$. As a result the transformations of eigenvectors via the σ -operator coincide with those defined by its corresponding spin operator. Therefore, all couplings will be constants and the Hamiltonian (2.3) will capture the same features as its Heisenberg parent.

(2) $s_{ij} \neq 0$ and $m_{ij} = 0$: The corresponding coefficient cannot be determined from Eq. (2.15a) and from eqs. (2.12b) and (2.15b) one obtains

$$a_{ij}^{s_{ij}, \pm 1} = a_{ij}^{s_{ij}, 0} = \pm 1. \quad (2.16)$$

We would like to point out that the “minus” sign is irrelevant to the case of two unpaired electrons.

(3) $s_{ij} = 0$: The associated parameter remains unconstrained and there exist a set of coefficients $c_{ij}^n \in \mathbb{R} \forall n \in \mathbb{N}$, such that

$$a_{ij}^{0,0} \in \{c_{ij}^n\}_{n \in \mathbb{N}}. \quad (2.17)$$

The values of c_{ij}^n depend on the number of unpaired valence electrons and intermediate nonmagnetic ions of the respective exchange bridges. Depending on the type of exchange these effective coefficients are functions of the Coulomb, hopping and exchange integrals. Thereby, for a linear cluster with only one bonding anion between magnetic cations and a unique electron's spatial distribution, one would obtain the limit $|c_{ij}^n - c_{ij}^k| \rightarrow 0, \forall n \neq k$, where $c_{ij}^n \rightarrow 1$. Accordingly, the changes in electron's distribution could be considered as negligible pointing to sharpened peaks in the magnetic spectrum. On the other hand, the inequality $|c_{ij}^n - c_{ij}^k| > 0$ for all $n \neq k$, would have to be considered as a sign for the presence of exchange paths of different energy, *i.e.* more than one favorable spatial distribution of unpaired electrons, and therefore of increased excitation width in energy. As an example, if i th and j th magnetic centers are linked via more than one exchange bridge of complex chemical structure, then one may expect that the exchange path is not unique. In such case according to (2.5) and (2.6) the transition energy reads

$$|\Delta E_n| = \sum_{\tau} \left| |c_{n,1}^{\tau}|^2 E_{1,M}^{\tau} - |c_{n,0}^{\tau}|^2 E_{0,0}^{\tau} \right|,$$

where n assigns a unique transition energy to a certain number of favorable spatial distributions. Hence, with Hamiltonian (2.3) and taking into account (2.17) we can express all existing transitions by

$$\Delta E_n = \frac{1}{2} J_{ij} (3c_{ij}^n \pm 1), \quad a_{ij}^{1,0} = \pm 1. \quad (2.18)$$

The set of values ΔE_n will correspond to a broadened peak in the magnetic spectrum. Applying the relation $\Delta E_n = 2J_{c_{ij}^n}$, where $J_{c_{ij}^n}$ is the n th value of the Heisenberg type exchange coupling from (2.18) we thus obtain

$$c_{ij}^n = \frac{4}{3} \frac{J_{c_{ij}^n}}{J_{ij}} \mp \frac{1}{3}, \quad a_{ij}^{1,0} = \pm 1. \quad (2.19)$$

As we will see later this approach allows one to explain in details the experimentally observed splitting and broadening of magnetic spectra in the molecular magnet $\text{Ni}_4\text{Mo}_{12}$, see e.g. FIG. 1.

III. THE TETRAMER $\text{Ni}_4\text{Mo}_{12}$

The indistinguishable spin-one Ni^{2+} ions of the spin cluster compound $\text{Ni}_4\text{Mo}_{12}$, are arranged on the vertices of a distorted tetrahedron, see FIG. 2. For this molecule the bonds Ni1-Ni2 and Ni3-Ni4 are slightly shorter about 0.03 Å than the other four³². Notice that the intermediate bridges contain ions of molybdenum, oxygen and hydrogen.

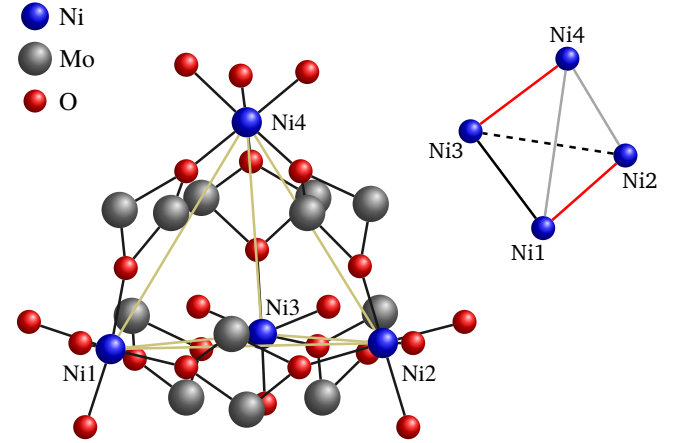


FIG. 2. Sketch of the structure of the molecular nanomagnet $\text{Ni}_4\text{Mo}_{12}$. The inset represents a schematic view of the arrangement of Ni ions (blue balls). The gray lines represent the two shorter distances, while the red lines show the effective spin-1 dimers.

To perform a thorough analysis of the magnetic excitations of the compound $\text{Ni}_4\text{Mo}_{12}$ obtained by INS experiments (see e.g. FIG. 1) reported in Ref.^{31,32} we employ Hamiltonian (2.3). Notice that the symmetry of the magnetic cluster imply $J_{ij} = J$ and further we assume that the magnetic centers Ni1-Ni2 and Ni3-Ni4 are coupled, which defines these bonds as the intersection of two different planes. Therefore, we have the total spin eigenstates $|s_{12}, s_{34}, s, m\rangle$, four $\hat{\sigma}$ operators for each constituent magnetic ion and two bond operators corresponding to both Ni1-Ni2 and Ni3-Ni4 spin pairs.

We point out that $\hat{\sigma}_1$ and $\hat{\sigma}_2$ are related with the Ni1-Ni2 pair that share the coefficients $a_{12}^{s_{12}, m_{12}}$ of the total bond $\hat{\sigma}_{12}$. The operators $\hat{\sigma}_3$ and $\hat{\sigma}_4$ are associated with the coefficient $a_{34}^{s_{34}, m_{34}}$ of $\hat{\sigma}_{34}$. Consequently from (2.3) we obtain the Hamiltonian

$$\begin{aligned} \hat{\mathcal{H}} = & J(\hat{\sigma}_1 \cdot \hat{\sigma}_2 + \hat{\sigma}_2 \cdot \hat{\sigma}_1 + \hat{\sigma}_3 \cdot \hat{\sigma}_4 + \hat{\sigma}_4 \cdot \hat{\sigma}_3) \\ & + J(\hat{\sigma}_{12} \cdot \hat{\sigma}_{34} + \hat{\sigma}_{34} \cdot \hat{\sigma}_{12}). \end{aligned} \quad (3.1)$$

With the applied effective spin-one spins the tetramer exhibits in total eighty one eigenstates without taking into account the quadrupolar, octupolar and other eigenfunctions related with higher symmetries. The ground state

of this nanomagnet is a singlet with possible eigenstates $\{|0,0,0,0\rangle, |1,1,0,0\rangle, |2,2,0,0\rangle\}$. On the other hand, the selection rules imply that the ground state excitations must be related with singlet-triplet transitions and since the quantum numbers s_{14} and s_{23} cannot be simultaneously varied, we deduce that the ground state is, related to the formation of two local triplets, i.e. $s_{14} = 1$ and $s_{23} = 1$. The triplet eigenstates are eighteen. Those, three in total, characterized by the local quintets $s_{14} = 2$ and $s_{23} = 2$ are not adequate to the established selection rules and nine are directly connected to experimental spectra.

A. Energy levels

According to the selected coupling scheme we denote the eigenvalues of (3.1) by $E_{s_{12}, s_{34}, s}^m$. The ground state is the singlet $|1,1,0,0\rangle$. Therefore, using (2.15) we get $a_{12}^{1,m_{12}} = a_{34}^{1,m_{34}} = 1$ and taking into account (3.1) we obtain

$$E_{1,1,0}^0 = -8J.$$

With the triplet eigenstates $|0,1,1,m\rangle$, $m_{34} \equiv m = 0, \pm 1$, the spins of Ni1 and Ni2 ions are coupled in singlet, the parameter $a_{12}^{0,0}$ remains unconstrained and can be determined using INS experimental data. For the corresponding energies we get

$$E_{0,1,1}^m = -2Ja_{34}^{1,m} - 4Ja_{12}^{0,0}, \quad m = 0, \pm 1,$$

where according to (2.16) we have $a_{34}^{1,0} = \pm 1$. Analyzing the $\text{Ni}_4\text{Mo}_{12}$ spectrum we further obtain $a_{12}^{0,0} \in \{c_{12}^1, c_{12}^2\}$.

When the singlet bond is Ni3-Ni4 the eigenstates are $|1,0,1,m\rangle$, $m_{12} \equiv m = 0, \pm 1$, the value of $a_{34}^{0,0}$ remains unconstrained and according to (3.1) we have

$$E_{1,0,1}^m = -2Ja_{12}^{1,m} - 4Ja_{34}^{0,0}, \quad m = 0, \pm 1,$$

where $a_{12}^{1,0} = \pm 1$. Without loss of generality we set $a_{34}^{0,0} = c_{34}$.

For all remaining triplets, i.e. $|1,1,1,m\rangle$, $|2,2,1,m\rangle$, $|2,1,1,m\rangle$ and $|1,2,1,m\rangle$, where $m = 0, \pm 1$, the corresponding coefficient are constrained, $a_{12}^{s_{12}, m_{12}} = 1$ and $a_{34}^{s_{34}, m_{23}} = 1$. Thus, we obtain

$$E_{1,1,1}^m = E_{2,2,1}^m = E_{2,1,1}^m = E_{1,2,1}^m = -6J.$$

The tetramer $\text{Ni}_4\text{Mo}_{12}$ exhibits also a singlet bond at the quintet level. The energies associated with the Ni1-Ni2 singlet bond and eigenstates $|0,2,2,m\rangle$, where $m_{34} \equiv m$ are

$$E_{0,2,2}^m = 2Ja_{34}^{2,m} - 4Ja_{12}^{0,0}, \quad m = 0, \pm 1, \pm 2,$$

where, the coefficients are determined by $a_{34}^{2,0} = \pm 1$ and $a_{12}^{0,0} \in \{c_{12}^1, c_{12}^2\}$.

Similarly, if the spins of third and fourth ions are in a singlet state, where the corresponding eigenstates are $|2,0,2,m\rangle$, then the Hamiltonian in (3.1) yield the following energy values

$$E_{2,0,2}^m = 2Ja_{12}^{2,m} - 4Ja_{34}^{0,0}, \quad m = 0, \pm 1, \pm 2,$$

where $a_{12}^{2,0} = \pm 1$.

With respect to the other twelve quintet eigenstates the coefficients $a_{12}^{s_{12}, m_{12}} = a_{34}^{s_{34}, m_{34}} = 1$ and therefore,

$$E_{2,2,2}^m = E_{1,1,2}^m = E_{2,1,2}^m = E_{1,2,2}^m = -2J.$$

For the remaining two levels we obtain $a_{12}^{s_{12}, m_{12}} = 1$ and $a_{34}^{s_{34}, m_{34}} = 1$. The energy sequence follows the Landé interval rule $E_{s+1} - E_s = 2Js$, see e.g. FIG. 3. The septet level is twenty one fold degenerate and it is defined by the eigenstates $|2,1,3,m\rangle, |1,2,3,m\rangle, |2,2,3,m\rangle$ with $m = 0, \pm 1, \pm 2, \pm 3$. All corresponding energies have equal value

$$E_{2,1,3}^m = E_{1,2,3}^m = E_{2,2,3}^m = 4J.$$

Applying the nonet state $|2,2,4,m\rangle$, where $m = 0, \dots, \pm 4$ we end up with $E_{2,2,4}^m = 12J$.

The described energy level structure is illustrated on FIG. 3. In what follows we find the following notations more convenient

$$\begin{aligned} E_0 &= -8J, & E_1 &= -2J - 4Jc_{12}^1, \\ E_2 &= -2J - 4Jc_{12}^2, & E_3 &= -2J - 4Jc_{34}, \\ E_4 &= -6J, & E_5 &= 2J - 4Jc_{12}^1, \\ E_6 &= 2J - 4Jc_{12}^2, & E_7 &= 2J - 4Jc_{34}, \\ E_8 &= -2J, & E_9 &= 4J, \\ E_{10} &= 12J. \end{aligned}$$

B. Scattering Intensities

The INS selection rules are $\Delta s = 0, \pm 1$, $\Delta m = 0, \pm 1$ and $\Delta s_{12} = 0, \pm 1$, $\Delta s_{34} = 0, \pm 1$. Here the transitions $\Delta s_{12} \neq 0$ and $\Delta s_{34} \neq 0$ are not allowed simultaneously. Within the applied coupling scheme we obtain $S^{\alpha\beta}(\mathbf{q}, \omega_{n'n}) + S^{\beta\alpha}(\mathbf{q}, \omega_{n'n}) = 0$, $\forall n, n', \alpha \neq \beta$ and $\sum_{\alpha} \Theta^{\alpha\alpha} = 2$. The energy of the first experimental magnetic excitation is approximately 0.4 meV. The corresponding peak is depicted on FIG. 1, see also³². This excitation is related with the transition between the ground state and the local singlet state $|0,1,1, \pm 1\rangle$. The associated scattering functions are

$$S^{\alpha\alpha}(\mathbf{q}, \omega_{10}) = \frac{4}{9}[1 - \cos(\mathbf{q} \cdot \mathbf{r}_{12})]p_0, \quad S^{zz}(\mathbf{q}, \omega_{10}) = 0, \quad (3.2)$$

where p_n is the population factor and $\alpha = x, y$. The magnetic excitation at 0.6 meV shown on FIG. 1 is associated with the eigenstate $|1,0,1, \pm 1\rangle$ and the scattering functions

$$S^{\alpha\alpha}(\mathbf{q}, \omega_{30}) = \frac{4}{9}[1 - \cos(\mathbf{q} \cdot \mathbf{r}_{34})]p_0, \quad S^{zz}(\mathbf{q}, \omega_{30}) = 0, \quad (3.3)$$

where $\alpha = x, y$. The functions (3.2) differ from (3.3) due to the spatial orientations of the spin bonds with $\mathbf{r}_{12} \cdot \mathbf{r}_{34} = 0$. For the same reason, we deduce that the third cold peak at 1.7 meV, see FIG. 1, is related with the transition between the ground state and non magnetic triplet $|0,1,1,0\rangle$. For $\alpha = x, y$ the corresponding scattering functions read

$$S^{zz}(\mathbf{q}, \omega_{50}) = \frac{4}{9}[1 - \cos(\mathbf{q} \cdot \mathbf{r}_{12})]p_0, \quad S^{\alpha\alpha}(\mathbf{q}, \omega_{50}) = 0.$$

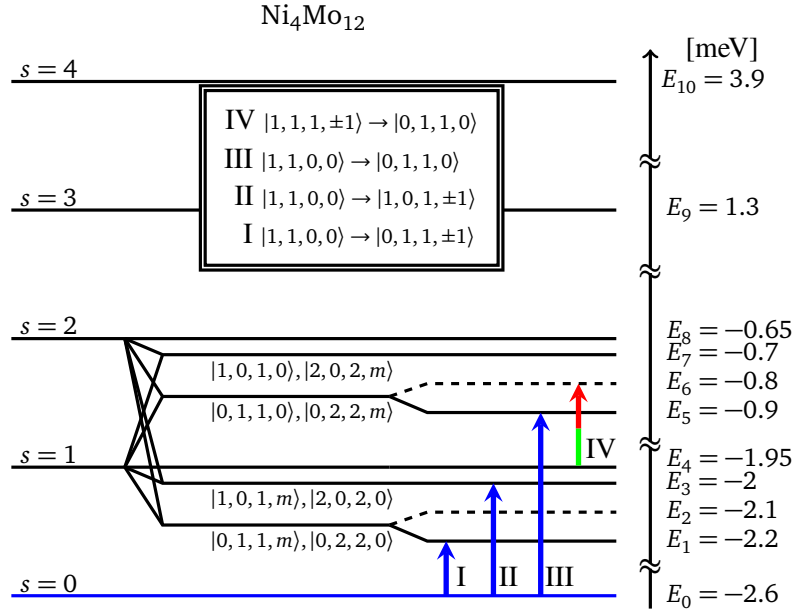


FIG. 3. Energy level structure and the corresponding transitions of $\text{Ni}_4\text{Mo}_{12}$. The blue line and arrows stands for the ground state energy and the ground state excitations, respectively. The red arrow marks the excited transition and the corresponding initial level is shown in red. The dashed lines represent the centers of the two bands. All transitions are denoted with respect to the experimental data shown on FIG. 1 provided from Ref.³¹.

The excited magnetic transition at around 1.2 meV shown by green and red items on FIG. 1 is nicely reproduced by the scattering functions

$$S^{\alpha\alpha}(\mathbf{q}, \omega_{64}) = \frac{2}{3}[1 - \cos(\mathbf{q} \cdot \mathbf{r}_{12})]p_4, \quad S^{zz}(\mathbf{q}, \omega_{64}) = 0,$$

where $\alpha = x, y$. The initial state is given by the triplet state $|1, 1, 1, \pm 1\rangle$ with two triplet bonds and the final one appears to be $|0, 1, 1, 0\rangle$. Hence if the neutron scatters from the Ni3-Ni4 dimer, then we have $\mathbf{q} \cdot \mathbf{r}_{12} = 0$ and $\mathbf{q} \cdot \mathbf{r}_{34} > 0$. Nevertheless, with the coefficients $a_{12}^{s_{12}, m_{12}}$ and $a_{34}^{s_{34}, m_{34}}$ one can uniquely identify the two spin bonds and distinguish I_{10} from I_{30} . Moreover, one can distinguish the eigenvalues of tetramer Hamiltonian corresponding to $m = 0$ and $m \neq 0$, with $S^{zz}(\mathbf{q}, \omega_{n'n}) = 0$ and $S^{xx}(\mathbf{q}, \omega_{n'n}) = 0$, $S^{yy}(\mathbf{q}, \omega_{n'n}) = 0$, respectively. This affects directly the integrated intensities, such that choosing $\mathbf{r}_{12} = (0, 0, r^z)$ and $\mathbf{r}_{34} = (r^x, 0, 0)$ from (2.1) yields

$$\begin{aligned} I_{10} &\propto \gamma_{10} \left[1 - \frac{\sin(qr)}{qr} \right] F^2(q), \\ I_{30} &\propto \gamma_{30} \left[1 - 6 \frac{\sin(qr)}{5(qr)^3} - 3 \frac{\sin(qr)}{5qr} + 6 \frac{\cos(qr)}{5(qr)^2} \right] F^2(q), \\ I_{50} &\propto \gamma_{50} \left[1 - 3 \frac{\sin(qr)}{(qr)^3} + 3 \frac{\cos(qr)}{(qr)^2} \right] F^2(q), \\ I_{64} &\propto \gamma_{64} \left[1 - \frac{\sin(qr)}{qr} \right] F^2(q), \end{aligned}$$

where

$$\gamma_{10} = \frac{8}{9}p_0, \quad \gamma_{30} = \frac{20}{27}p_0, \quad \gamma_{50} = \frac{8}{27}p_0, \quad \gamma_{64} = \frac{4}{3}p_4,$$

and $r = |\mathbf{r}_{12}| = |\mathbf{r}_{34}|$. The integrated intensities as a function of temperature are shown on FIG. 4. According to Ref.³² the average distance between Ni-Ni ions is $r = 6.68 \text{ \AA}$. The magnitude of the scattering vector is fixed at $q = 1 \text{ \AA}^{-1}$ and the calculated form factor for Ni^{2+} di-cations is $F(q) = 256(16 + q^2 r_0^2)^{-2}$, where $r_0 = 0.529 \text{ \AA}$ is the Bohr radius. The dependence of normalized intensities, $I_{n'n} \rightarrow I_{n'n}/\gamma_{n'n}$, on the scattering vector is shown on FIG. 5.

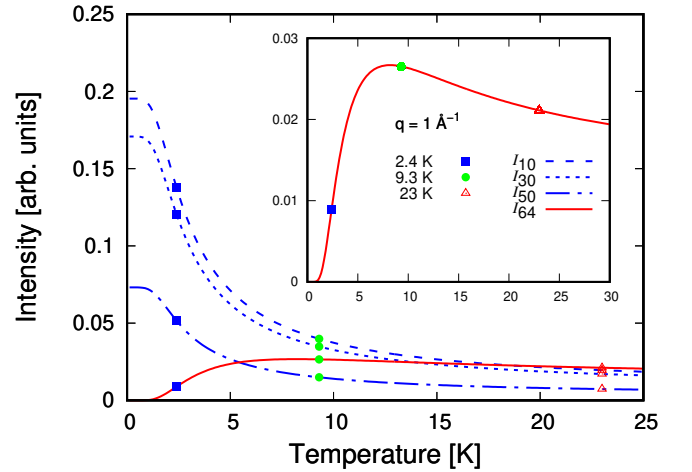


FIG. 4. Intensities as a function of the absolute temperature. I_{10} , I_{30} and I_{50} correspond to the ground state transitions with energies 0.4 meV, 0.6 meV and 1.7 meV, respectively. The intensity I_{64} in the inset stands for the excited transition with energy 1.15 meV. The blue squares, the green circles and red triangles point to the values of intensities in table 1.

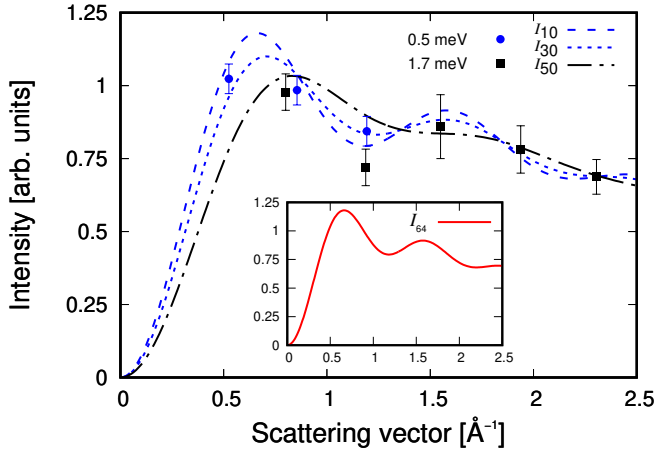


FIG. 5. Normalized by $\gamma_{n'n}$ intensities as a function of the scattering vector along with the experimental data of Ref.³². I_{10} , I_{30} and I_{50} correspond to ground state transitions with energies 0.4 meV, 0.6 meV and 1.7 meV, respectively. The intensity I_{64} stands for the excited transition with energy 1.15 meV. The inset shows the intensity I_{64} that coincides with the function I_{10} .

TABLE 1. Calculated values of integrated intensities $I_{n'n}$ [arb. units] at temperatures 2.4, 9.3 and 23 K, shown on FIG. 4 as blue squares, green circles and red triangles, respectively.

Transitions	I	II	III	IV
Intensities	I_{10}	I_{30}	I_{50}	I_{64}
2.4 [K]	0.137(6)	0.120(3)	0.051(5)	0.008(9)
9.3 [K]	0.039(8)	0.034(8)	0.014(9)	0.026(5)
23 [K]	0.019(5)	0.017(1)	0.007(3)	0.021(1)

C. Energy of the magnetic transitions

The energy transition E_{ij} between i th and j th levels, corresponding to the calculated scattering intensities are

$$\begin{aligned} E_{10} &= 6J - 4Jc_{12}^1, & E_{30} &= 6J - 4Jc_{34}, \\ E_{50} &= 10J - 4Jc_{12}^1, & E_{64} &= 8J - 4Jc_{12}^2. \end{aligned} \quad (3.4)$$

From the last equations we can take advantage of one more constraint to determine J , $E_{50} - E_{10} = 4J$. According to the experimental data^{31,32} the ground state magnetic excitations are grouped in two relatively broadened peaks. The first peak is centered at about 0.5 meV and the second one at 1.7 meV. Furthermore, the first peak is composed of two subbands with energies $E_{10} = 0.4$ meV and $E_{30} = 0.6$ meV. The width of the second peak can be explained by the presence of an energy band, where the transition energies are restricted in the region

TABLE 2. Values of the coupling constants and the quantities c_{12}^1 , c_{12}^2 and c_{34} for all magnetic excitations with energies given in eq. (3.4). The results are obtained by taking into account the experimental data of Ref.^{31,32}.

Transitions	I	II	III	IV
$E_{n'n}$ [meV]	E_{10}	E_{30}	E_{50}	E_{64}
	0.4	0.6	1.7	1.15
J [meV]	0.325	0.325	0.325	0.325
$J_{c_{12}^1}$ [meV]	0.372	—	0.372	—
$J_{c_{12}^2}$ [meV]	—	—	—	0.353
$J_{c_{34}}$ [meV]	—	0.334	—	—
c_{12}^1	1.1923	—	1.1923	—
c_{12}^2	—	—	—	1.1153
c_{34}	—	1.0384	—	—

1.6 meV to 1.8 meV. Therefore, setting $E_{50} = 1.7$ meV we obtain $E_{50} - E_{10} = 1.3$ meV and $J = 0.325$ meV. The computed energy transitions are depicted on FIG. 3. The centers of both energy bands referring to the value $c_{12}^2 = 1.1153$ are shown by dashed lines. The energies of all transitions and the corresponding parameters are given in table 2.

IV. CONCLUSION

We propose a formalism for exploring the physical properties of molecular magnets with non trivial bridging structure. The underlying concept lies on the hypothesis that due the cluster symmetry, as well as its shape, size and the chemical structure that surrounds the magnetic ions, the spatial distribution of valence electrons is not unique leading to a variation of the relevant Coulomb, hopping and direct exchange energies.

Studying the INS spectra of the compound $\text{Ni}_4\text{Mo}_{12}$ with the Hamiltonian (2.3) we were able to derive a detailed picture for the neutron scattering intensities FIG. 4 and FIG. 5. Hamiltonian (3.1) leads to energy spectrum with two energy bands, shown in FIG. 3. These bands are related to the fact that the tetramer cluster exhibits two distinguishable with respect to the coefficients $a_{12}^{s_{12}, m_{12}}$ and $a_{34}^{s_{34}, m_{34}}$ bonds. We ascribe this feature to the difference in the chemical environment around Ni1-Ni2 and Ni3-Ni4 couples that give rise to distinct spatial distributions of the valence electrons. This allowed a unique identification of the magnetic excitations. Thereby, the obtained energy bands explain the width of second ground state peaks centered at 1.7 meV and the splitting of the first one centered at 0.5 meV. In particular, for $s_{12} = 0$, $s_{34} = 0$ and $i = 1, 2$ we get $|c_{12}^i| > 1$ and $|c_{34}| > 1$, respectively. Besides, according to (2.19) we have $J < J_{c_{12}^i}$ and $J < J_{c_{34}}$, see table 2. These inequalities signals that the strength of the exchange is amplified. Furthermore, the inequality $J_{c_{34}} < J_{c_{12}^i}$ indicates that

most probably the density of electrons along Ni3-Ni4 bond is lower than that along the Ni1-Ni2.

To conclude we would like to anticipate that the results for the magnetization and low-field magnetic field susceptibility of the tetramer $\text{Ni}_4\text{Mo}_{12}$ are in concert with the experimental measurements. These results will be the subject of a separate paper.

ACKNOWLEDGMENT

The authors are indebted to Prof. N.S. Tonchev and Prof. N. Ivanov for the very helpful discussions and to Prof. J. Schnack

for providing us the experimental results on FIG. 1. This work was supported by the Bulgarian National Science Fund under contract DN/08/18.

-
- * mgeorgiev@issp.bas.bg
- ¹ E. Roduner, *Nanoscope Materials : Size-Dependent Phenomena* (The Royal Society of Chemistry, 2006).
 - ² H. Chamati, "Theory of Phase Transitions: From Magnets to Biomembranes," *Adv. Planar Lipid Bilayers Liposomes* **17**, 237 (2013).
 - ³ D. J. Sellmyer, B. Balamurugan, B. Das, P. Mukherjee, R. Skomski, and G. C. Hadjipanayis, "Novel structures and physics of nanomagnets," *J. Appl. Phys.* **117**, 172609 (2015).
 - ⁴ B. Sieklucka and D. Pinkowicz, eds., *Molecular Magnetic Materials: Concepts and Applications* (Wiley, Weinheim, 2017).
 - ⁵ J. B. Goodenough, "Theory of the Role of Covalence in the Perovskite-Type Manganites $[\text{La}, \text{M}(\text{II})]\text{MnO}_3$," *Phys. Rev.* **100**, 564–573 (1955).
 - ⁶ G. C. DeFotis, E. D. Remy, and C. W. Scherrer, "Magnetic and structural properties of $\text{Mn}(\text{SCN})_2(\text{CH}_3\text{OH})_2$: A quasi-two-dimensional Heisenberg antiferromagnet," *Phys. Rev. B* **41**, 9074 (1990).
 - ⁷ N. A. Law, J. W. Kampf, and V. L. Pecoraro, "A magneto-structural correlation between the Heisenberg constant, J , and the Mn-O-Mn angle in $[\text{Mn}^{\text{IV}}(\mu\text{-O})]_2$ dimers," *Inorg. Chim. Acta* **297**, 252 (2000).
 - ⁸ M. J. Han, T. Ozaki, and J. Yu, "Electronic structure, magnetic interactions, and the role of ligands in Mn_n ($n=4,12$) single-molecule magnets," *Phys. Rev. B* **70**, 184421 (2004).
 - ⁹ N.J. Perks, R.D. Johnson, C. Martin, L.C. Chapon, and P.G. Radaelli, "Magneto-orbital helices as a route to coupling magnetism and ferroelectricity in multiferroic $\text{CaMn}_7\text{O}_{12}$," *Nat. Commun.* **3**, 1277 (2012).
 - ¹⁰ T. Gupta and G. Rajaraman, "Modelling spin Hamiltonian parameters of molecular nanomagnets," *Chem. Com.* **52**, 8972 (2016).
 - ¹¹ M. M. Hänninen, A. J. Mota, R. Sillanpää, S. Dey, G. Velmurugan, G. Rajaraman, and E. Colacio, "Magneto-Structural Properties and Theoretical Studies of a Family of Simple Heterodinuclear Phenoxide/Alkoxide Bridged $\text{Mn}^{\text{III}}\text{Ln}^{\text{III}}$ Complexes: On the Nature of the Magnetic Exchange and Magnetic Anisotropy," *Inorg. Chem.* **57**, 3683 (2018).
 - ¹² C. Loose, E. Ruiz, B. Kersting, and J. Kortus, "Magnetic exchange interaction in triply bridged dinickel(II) complexes," *Chem. Phys. Lett.* **452**, 38 (2008).
 - ¹³ A. Panja, N. Ch. Jana, S. Adak, P. Brandão, L. Dlhán, J. Titiš, and R. Boča, "The structure and magnetism of mono- and di-nuclear Ni(II) complexes derived from $\{\text{N}_3\text{O}\}$ -donor Schiff base ligands," *New J. Chem.* **41**, 3143 (2017).
 - ¹⁴ A. Das, K. Bhattacharya, S. Giri, and A. Ghosh, "Synthesis, crystal structure and magnetic properties of a dinuclear and a trinuclear Ni(II) complexes derived from tetradentate ONNO donor Mannich base ligands," *Polyhedron* **134**, 295 (2017).
 - ¹⁵ T. J. Woods, H. D. Stout, B. S. Dolinar, K. R. Vignesh, M. F. Ballesteros-Rivas, C. Achim, and K. R. Dunbar, "Strong Ferromagnetic Exchange Coupling Mediated by a Bridging Tetrazine Radical in a Dinuclear Nickel Complex," *Inorg. Chem.* **56**, 12094 (2017).
 - ¹⁶ R. A. Klemm and D. V. Efremov, "Single-ion and exchange anisotropy effects and multiferroic behavior in high-symmetry tetramer single-molecule magnets," *Phys. Rev. B* **77**, 184410 (2008).
 - ¹⁷ W. Hübner, Y. Pavlyukh, G. Lefkidis, and J. Berakdar, "Magnetism of a four-center transition-metal cluster revisited," *Phys. Rev. B* **96** (2017).
 - ¹⁸ S. W. Lovesey, *Theory of Neutron Scattering from Condensed Matter: Polarization Effects and Magnetic Scattering*, International Series of Monographs on Physics, Vol. 2 (Oxford University Press, Oxford, New York, 1986).
 - ¹⁹ M. F. Collins, *Magnetic critical scattering*, Oxford Series on Neutron Scattering in Condensed Matter (Oxford University, New York, 1989).
 - ²⁰ A. Furrer, J. Mesot, and T. Strässle, *Neutron Scattering in Condensed Matter Physics*, Series on Neutron Techniques and Applications (World Scientific, 2009).
 - ²¹ B. P. Toperverg and H. Zabel, "Neutron Scattering in Nanomagnetism," in *Neutron Scattering - Magnetic and Quantum Phenomena*, Experimental Methods in the Physical Sciences, Vol. 48, edited by F. Fernandez-Alonso and D. L. Price (Elsevier, 2015) p. 339.
 - ²² A. Stebler, H. U. Guedel, A. Furrer, and J. K. Kjems, "Intra- and intermolecular interactions in $[\text{Ni}_2(\text{ND}_2\text{C}_2\text{H}_2\text{ND}_2)_4\text{Br}_2]\text{Br}_2$. Study by inelastic neutron scattering and magnetic measurements," *Inorg. Chem.* **21**, 380 (1982).
 - ²³ M. Azuma, T. Odaka, M. Takano, D. A. Vander Griend, K. R. Poeppelmeier, Y. Narumi, K. Kindo, Y. Mizuno, and S. Maekawa, "Antiferromagnetic ordering of $S = \frac{1}{2}$ triangles in $\text{La}_4\text{Cu}_3\text{MoO}_{12}$," *Phys. Rev. B* **62**, R3588 (2000).
 - ²⁴ J. Ummethum, J. Nehrkorn, S. Mukherjee, N. B. Ivanov, S. Stüiber, Th. Strässle, P. L. W. Tregenna-Piggott, H. Mutka, G. Christou, O. Waldmann, and J. Schnack, "Discrete antiferromagnetic spin-wave excitations in the giant ferric wheel Fe_{18} ," *Phys. Rev. B* **86**, 104403 (2012).

- ²⁵ H. Kageyama, M. Nishi, N. Aso, K. Onizuka, T. Yoshida, K. Nukui, K. Kodama, K. Kakurai, and Y. Ueda, "Direct Evidence for the Localized Single-Triplet Excitations and the Dispersive Multitriplet Excitations in $\text{SrCu}_2(\text{BO}_3)_2$," *Phys. Rev. Lett.* **84**, 5876 (2000).
- ²⁶ B. D. Gaulin, S. H. Lee, S. Haravifard, J. P. Castellan, A. J. Berlinsky, H. A. Dabkowska, Y. Qiu, and J. R. D. Copley, "High-Resolution Study of Spin Excitations in the Singlet Ground State of $\text{SrCu}_2(\text{BO}_3)_2$," *Phys. Rev. Lett.* **93**, 267202 (2004).
- ²⁷ V. O. Garlea, S. E. Nagler, J. L. Zarestky, C. Stassis, D. Vaknin, P. Kögerler, D. F. McMorro, C. Niedermayer, D. A. Tennant, B. Lake, Y. Qiu, M. Exler, J. Schnack, and M. Luban, "Probing spin frustration in high-symmetry magnetic nanomolecules by inelastic neutron scattering," *Phys. Rev. B* **73**, 024414 (2006).
- ²⁸ D. Vaknin and F. Demmel, "Magnetic spectra in the tridimensional-icosahedron Fe_9 nanocluster by inelastic neutron scattering," *Phys. Rev. B* **89**, 180411 (2014).
- ²⁹ M. Georgiev and H. Chamati, "Magnetic excitations in the trimeric compounds $\text{A}_3\text{Cu}_3(\text{PO}_4)_4$ ($\text{A} = \text{Ca}, \text{Sr}, \text{Pb}$)," *C.R. Acad. Bulg. Sci.* **72**, 29 (2019).
- ³⁰ A. Müller, C. Beugholt, P. Kögerler, H. Bögge, S. Bud'ko, and M. Luban, "[$\text{Mo}_{12}^{\text{V}}\text{O}_{30}(\mu_2\text{-OH})_{10}\text{H}_2\{\text{Ni}^{\text{II}}(\text{H}_2\text{O})_3\}_4$], a Highly Symmetrical ε -Keggin Unit Capped with Four Ni^{II} Centers: Synthesis and Magnetism," *Inorg. Chem.* **39**, 5176 (2000).
- ³¹ J. Nehr Korn, M. Höck, M. Brüger, H. Mutka, J. Schnack, and O. Waldmann, "Inelastic neutron scattering study and Hubbard model description of the antiferromagnetic tetrahedral molecule $\text{Ni}_4\text{Mo}_{12}$," *Eur. Phys. J. B* **73**, 515 (2010).
- ³² A. Furrer, K. W. Krämer, Th. Strässle, D. Biner, J. Hauser, and H. U. Güdel, "Magnetic and neutron spectroscopic properties of the tetrameric nickel compound $[\text{Mo}_{12}\text{O}_{28}(\mu_2\text{-OH})_9(\mu_2\text{-OH})_3\{\text{Ni}(\text{H}_2\text{O})_3\}_4] \cdot 13\text{H}_2\text{O}$," *Phys. Rev. B* **81**, 214437 (2010).
- ³³ J. Jensen and A. R. Mackintosh, *Rare Earth Magnetism : Structures and Excitations*, International Series of Monographs on Physics, Vol. 81 (Clarendon, Oxford; New York, 1991).
- ³⁴ M. Georgiev and H. Chamati, "Magnetic Exchange in Spin Clusters," AIP Conf. Proc. (2018), in press, [arXiv:1811.12881](https://arxiv.org/abs/1811.12881) [physics.atm-clus].
- ³⁵ I. Fleming, *Molecular Orbitals and Organic Chemical Reactions* (Wiley, Chichester, UK, 2009).
- ³⁶ Björn O. Roos, "The Complete Active Space Self-Consistent Field Method and its Applications in Electronic Structure Calculations," in *Advances in Chemical Physics*, edited by K. P. Lawley (John Wiley & Sons, Inc., Hoboken, NJ, USA, 2007) pp. 399–445.
- ³⁷ P. G. Szalay, T. Müller, G. Gidofalvi, H. Lischka, and R. Shepard, "Multiconfiguration Self-Consistent Field and Multireference Configuration Interaction Methods and Applications," *Chem. Rev.* **112**, 108–181 (2012).